



A Review of Broadband Microfabricated Ultrasonic Systems for Biomedical Applications

R. Yu. Kostyuk^f,  [0009-0006-9575-2599](https://orcid.org/0009-0006-9575-2599)

S. A. Naida^s, Dr.Sc.(Eng.) Prof,  [0000-0002-5060-2929](https://orcid.org/0000-0002-5060-2929)

National Technical University of Ukraine "Igor Sikorsky Kyiv Polytechnic Institute"  [00syn5v21](https://doi.org/10.20535/2523-4455.me.303514)
Kyiv, Ukraine

Abstract—Starting from an overview of historical aspects of biomedical ultrasound development and its application areas, as well as the brief description of state-of-the art microfabrication technologies, used for capacitive and piezoelectrical micromachined ultrasonic transducers manufacturing, also outlining their modelling approaches, the reader will be further presented with an overview of existing methods for achieving broadband operation both at unit transducer and transducers array levels. Moreover, a generalized signal processing system is discussed, including description of known approaches for building blocks implementation in analog, digital and mixed-signal domains (such as drivers, amplifiers, ADCs, etc.).

Keywords — *biomedical ultrasound; wideband transducers; micromachined ultrasonic transducers (MUTs); CMUT; PMUT; ASIC; CMOS.*

I. INTRODUCTION

Usage of ultrasound (US) in medical industry has been intensively developed over last eight decades, starting from the late 1940s, when the First International Congress of Ultrasound in Medicine took place [1].

From a medical perspective, the variety of health care applications includes wide range of diseases that can be treated by ultrasound means. In particular, they encompass physical diagnostic imaging [2], orbital hemodynamics in ophthalmology [3], intravascular imaging in cardiology [4], hearing assessment [5], oncology [6], obstetrics and gynecology [7], [8], endoscopic gastroenterology [9], anesthesiology [10], neonatology [11] and others.

Technologies, that are used in medical ultrasound, were moving forward from simple one-dimensional A-mode scanners [12] to more informative imaging systems incorporating B- (2D), C- (3D), M- (motional) scan modes [13]–[15], as well as ultrafast, superresolution [16] and Doppler [17] imaging. Moreover, device miniaturization becomes possible due to the elaboration of high-end technologies [18], which results in development of flexible wearable [19] and implantable medical ultrasound sensors [20].

Different piezoelectric materials [21] became a standard in medical ultrasound since the first reported usage of piezoelectric effect in quartz crystal transducer acting as a head scanner [22]. The number of peculiarities is inherent in this technology, including impedance matching [23] and the constant pursuit for a wide operating frequency range [24], [25]. The former results in power

losses during acoustic energy transfer, because significant amounts of energy are reflecting into transducer, whereas the latter is crucial for axial or lateral resolution and, as a result, in more detailed structural description of lesions or anatomical peculiarities of human organs [26]. Another aspect is the compatibility with biological tissues, which results in tremendous number of invented synthetic piezoceramic materials [27]. Also, it should be noted that despite of abovementioned, piezoceramic devices are usually bulky and fabrication of tiny medical transducers becomes complex [28], [29].

In parallel with the expansion of piezoelectric materials, the capabilities of microelectronic fabrication were also enhanced, which caused a breakthrough in ultrasound transducers development by inventing so called micromachined ultrasonic transducers (MUTs), which in turn was the further evolution of already known microelectromechanical systems (MEMS) [30]. MUTs are the promising technology which can help to achieve a number of advantages comparing to conventional piezoceramic devices, such as compatibility with application specific integrated circuit (ASIC) platforms [31], [32], and as a result a high reliability of the system, which becomes crucial in fabrication of medical equipment in terms of high-yield perspective and minimization of biological safety related issues [33]. They also provide the possibility to decrease power consumption of the system by using sophisticated power-efficient processing circuitry [34], and improve impedance matching, because MUTs inherently act as a membranes, comparing to usual bulk piezoceramic transducers. Another advantage of MUTs,



is that they have better matching between the elements of ultrasound array just because of precise fabrication technologies.

In general, biomedical ultrasound electro-acoustical system, which firstly produces excitation acoustic signal and then handles the reflected signal, consists of transducers array, analog front-end (AFE) and digital back-end (DBE) stages [35]. The former serves for power pumping in transmitter (Tx) mode and signal preconditioning in receiver mode (Rx), while the latter is used to control AFE and implements digital signal processing algorithm. Different parts of overall system can be IC-based or FPGA-based, depending on application needs [36]. The application of machine learning processing algorithms for overcoming a transmitter-receiver alignment issue is also developing [37].

This paper aims to examine the principles of micromachined ultrasonic transducers' development and fabrication in the first section, following by a review of ASIC signal processing systems in the second section, focusing on the broadband operation for biomedical purposes.

II. MICROMACHINED ULTRASONIC TRANSDUCERS AND ARRAYS

A. MUT types

Nowadays, the two main types of MUTs exist — capacitive (CMUT) and piezoelectrical (PMUT) micromachined transducers. The operational principle of CMUT is based on modulation of Coulomb attraction force [38], [39], while the operation of PMUT depends solely on piezoelectrical effect. The core idea utilized in fabrication of both transducer types is to use the planar-based technology to create a vibrating membrane (usually a multilayer stack, especially for PMUTs), placed on insulated silicon substrate, with underlying cavity and different types of deposited metal electrodes (Fig. 1).

Typically, PMUT is a multilayer structure with matching and backing layers [40], while CMUT reminds a simple capacitor, which gives the latter an advantage in wider bandwidth [41], but with inherent nonlinearity of voltage to pressure transfer function [39], [42].

To describe the transmission or directivity behavior of PMUT and CMUT through the electrical, mechanical and acoustical domains, conventional equivalent circuits approach is used [43], [44], which is also supplemented by broadly adopted finite element method (FEM) verification (COMSOL, ANSYS) or optimized computational algorithms [45], as well as comprehensive analytical models [46] were derived. All of these models are completely depending on membrane geometry (square, rectangular, circular [47] — the latter is most often used in practice), presence of additional mechanical structures (cavities [43], Helmholtz resonators [48]) or various electrode types [46].

The main acoustical characteristics of both CMUTs and PMUTs are fractional bandwidth (FBW), measured at -3dB or -6dB level, displacement (m/V), transmitting (Pa/V) and receiving (V/Pa) sensitivities, which are typically defined in basic medias like air and water or special electric insulation fluids (Fluorinert FC-40 [43], FC-70 [49] or FC-84 [50] etc.). For PMUT, as for inherently piezoelectric material, critical parameters are electromechanical coupling coefficient, resonant and anti-resonant frequencies.

From the electrical side both PMUT or CMUT can be similarly modeled as electrical impedance, formed from a capacitance in parallel with a parasitic resistance, representing a dielectric loss caused by leakage currents [40], [51]. However, more precise electrical equivalent models exist, which include an additional inductance and capacitance [52]. PMUTs typically possess lower impedance, then usual bulk piezoelectric transducers, that stems from higher capacitance (tens of pF [53] comparing to hundreds of fF for CMUT [54]), which also gives less vulnerability to parasitic coupled capacitance [55]. Another difference between PMUTs and CMUTs is also in the value of DC biasing (polarization) voltage, which should be applied to create constant electric field in CMUTs (this voltage falls in range from tens to hundreds of volts [42], [44]), while PMUTs aren't required to be biased at all [56]. However, there is recent research in development of low-voltage CMUTs [57] with 12V of DC bias. Obviously, for both types of transducers, mechanical oscillations are caused only by AC excitation of their electrical inputs.

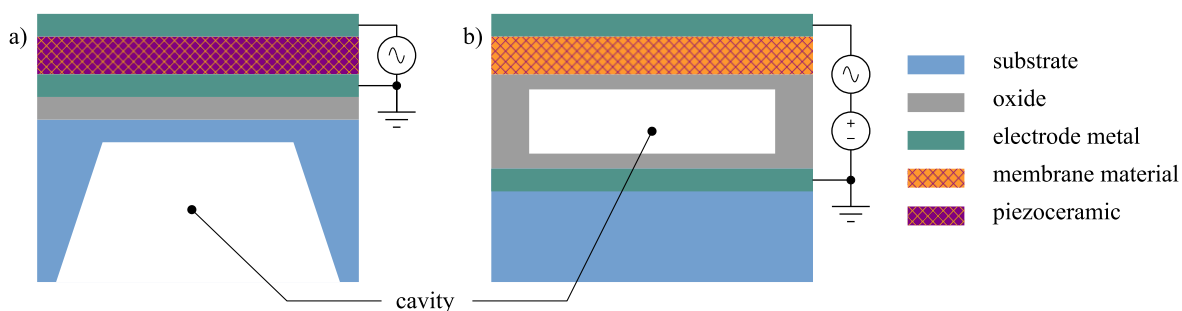


Fig. 1 Schematic cross-sections of basic PMUT (a) and CMUT (b) structures

Central frequency of CMUTs and PMUTs for medical applications falls in a range from a few to tens of megahertz [39], [58], [59]. However, the difference between the fractional bandwidths catches the eye: CMUTs are reported to operate with FBW of about 76% [57], and ~100% [60], while PMUTs are usually relatively narrow-band — 47.5% [43] and ~57% [61] FBWs.

Different techniques are implemented to increase PMUTs fractional bandwidth, which includes introduction of resonant cavities to the transducer structure [43], different electrode structures [43], usage of matching electrical network [50] or excitation on different vibration modes [41].

Another interesting approach is to implement resonant frequency tuning/switching, which gives more flexibility in designing the imaging system. This feature can be achieved by changing the biasing voltage [62] for CMUTs or activating different electrode sets [63] for PMUTs.

In conclusion, when comparing capacitive and piezoelectric transducers in terms of wideband biomedical applications, PMUTs have the advantage of low-voltage devices, which gives inherent safety and CMOS integration, while CMUTs, despite of their wideband behavior, either complicated to manufacture with extremely tiny gap between electrodes [57] or required to use high biasing voltage, and as a result — insulation from human's tissue require thorough fabrication techniques. Hence, the obvious trade-off between high-bandwidth and low-voltage appears.

B. *MUT fabrication*

Surface and bulk micromachining [64] allows to create layered mechanical structures (essentially MUTs) with base size of about tens to hundreds of microns on top of a silicon substrate. Fabrication methods are based on the photolithography process with appropriate mask design and also involves different techniques of material synthesis and processing [53], such as oxidation (dry or wet, proceeded at high temperature), wet (in potassium hydroxide (KOH) or hydrofluoric (HF) acid) or dry etching, physical vapor deposition (reactive, DC or RF sputtering), chemical vapor deposition, spin-on deposition (sol-gel method), polishing [51], followed by final steps of die separation and packaging.

Most common material for PMUT membrane is lead zirconate titanate PZT [53], [65]–[67], since it has high transmitting sensitivity [68], but on the other hand includes high temperature film deposition step, which can impact integration with CMOS technology [47]. However, materials with improved properties or optimized manufacturing processes were found, such as aluminum nitride (AlN) with high receiving sensitivity [68]), zinc oxide (ZNO) [69] for high frequency devices, potassium sodium niobate (KNN) [70] or even polyvinylidene

fluoride (PVDF) for flexible applications [71]. Some of these materials are intended to be lead-free to imply biological compatibility, though their characteristics are inferior compared to PZT. At the same time, CMUT membranes are made simply from silicon nitride or polymer [72], [73].

In general, fabrication steps of MUT structure creation involve silicon wafer (substrate) preparation, formation of underlying cavity, membrane film (or stack of films) deposition, formation of top and bottom electrodes, and the subsequent passivation (isolation) of the finalized structure to ensure, for example, immersive abilities of device. Several kinds of both CMUT and PMUT fabrication processes were developed, such as sacrificial layer release [74], different kinds of wafer bonding [75], front-side or back-side etching [76].

The main idea of sacrificial layer release process is to create a cavity on a single wafer by etching of previously deposited layers (silicon oxide, photoresist, or aluminum) [77], which is buried under membrane and the etching is processed via the small openings. On the other hand, wafer bonding intends to bond two separate wafers (the base one and the Silicon-On-Insulator (SOI) wafer — structure formed as a stack of thin top silicon layer, underlying buried oxide that placed on thick bottom silicon layer) with initially etched cavities. Wafer bonding process allows to define plate thickness and cavity height better than it is done with sacrificial layer release, but requires precise alignment and cleanliness of the wafers [75], [76].

Creation of PMUT structures can be achieved by another two techniques — front-side and back-side etching. The former implies the cavity formation from the top side of the wafer via the special etching hole, while the latter is typically proceeded at SOI wafer by etching the cavity in the bottom silicon layer [59], which is called deep reactive-ion etching (DRIE) process.

C. *MUT arrays*

Ultrasound imaging systems typically incorporate not just a single MUT but an entire array of them, integrated into an acoustic antenna, in order to convert electrical energy into mechanical energy, and then obtaining acoustic field with desired spatial directivity characteristic [78]. Described mode is a transmitting mode, while the reverse algorithm for converting energy from an acoustic field into electrical signals is called a reception mode. Most often a linear antenna is used, which is adapted to work as part of one-dimensional (1-D) [54] or two-dimensional (2-D) [51], [72], scanning (in lateral and axial directions) system. In such systems beamforming algorithms is accomplished via introduction of delay into transmitting or receiving electrical signals for each transducer in the array. MUT arrays also can be different in size (N×M), can have various transducer membrane dimensions, which are usually placed at a distance that creates

optimal element pitch (usually $\lambda/2$ [68]), aiming to minimize grating lobes of directivity characteristic. Further operation improvement can be achieved by introducing of complex multi-element channels (with several transducers in each) into overall array [67], [70]. Also, the arrays of specific annular shapes with high fill-factor were developed [55] for intravascular imaging. The comparison between different arrays characteristics is presented in Table 1.

Usage of transducer arrays instead of a single one can also give an advantage in obtaining a wider bandwidth. As reported, bandwidth expansion in MUT arrays can be attained in various ways, for example frequency compounding technique, which stems from the frequency spectrum overlapping of multiple transducers with different dome (PMUT membrane shape) dimensions [79]. Another approach is to form a channel from PMUTs with adjacent resonant frequencies (higher and lower), simultaneously incorporating the different polarization directions for each transducer type [80]. Also, bandwidth extension can be obtained by reducing membrane thickness [55] or by introducing more membrane damping with additional polyimide layer deposited onto PMUT membranes [58], as well as the similar approach was developed by adding the polydimethylsiloxane (PDMS) backing structure [66]. Optimization of layer stack fabrication to achieve broad FBW of 95.7% for PMUT super pixel array was also developed [70]. Moreover, simulations show severe impact of the fill-factor (ratio of MUT

active area to its total area) on the array wideband performance [54].

In addition, an important issue that requires attention while designing the MUT arrays is the cross-talk between array elements, which is caused by boundary Stoneley and elastic Lamb waves [38].

III. SIGNAL PROCESSING SYSTEMS

A. Basic AFE structure

Modern ultrasound imaging systems are usually implemented by using digital computational algorithms at the final processing step of received information. However, since ultrasound transducer generates analog signal and also have to be excited by analog signal, then analog circuits should be used as a first stage of interface between transducer and digital algorithm. Such functions are ensured by analog front-end (AFE) schematics, followed by analog-to-digital conversion (ADC), and finally processed by digital back-end (DBE) sub-system. Common structure of ultrasound data acquisition system is depicted in Fig. 2 [34], [49]. It consists of transducers array, transmit/receive (Tx/Rx) switch, transmit and receive channels' analog circuitries, analog-to-digital converter, and digital subsystem with Rx processing, Tx generation (can be digital-to-analog conversion (DAC) [81]) and beamform control algorithm, followed by human interface device(s).

TABLE 1 COMPARISON OF MUT ARRAYS

Reference number	[54]	[53]	[79]	[55]	[65]	[66]	[72]	[67]	[70]
Year	2004	2009	2012	2015	2019	2021	2022	2022	2024
Transducer type	CMUT	PMUT	PMUT	PMUT	PMUT	PMUT	CMUT	PMUT	PMUT
Membrane material	SiN _x	PZT	PNZT	AlN	PZT	PZT	Si	PZT	KNN
Membrane thickness*	0.4 μm	2 μm	–	0.75 μm	1.9 μm	1 μm	2 μm	1 μm	0.9 μm
Media	Water	–	Water	FC-70	Water	Water	Water	Water	FC-3283
Central frequency	30 MHz	1.88MHz	5 MHz	18.6 MHz	~6.75 MHz	15.6 MHz	3.8 MHz	1.5 MHz	4.7 MHz
Transmitting Bandwidth	–	–	55% –3dB	4.9 MHz –3dB	–	92% –6dB	–	184% –6dB	95.7% –6dB
Receiving Bandwidth	80% –6dB	–	–	–	~89%	–	110%	–	–
Transmitting sensitivity	–	–	85 kPa/V	9 kPa/V	–	–	–	430 Pa/V	3.8 kPa/V
Receiving sensitivity	–	–	–	–	~0.48 mV/kPa	–	–213 dB	190 mV/MPa	–
Array size	1×64	6×6	57	–	1 × 65	16 × 8	4 × 16	1×128	1×32
Number of transducers	7040	36	–	1261	3900	128	2240	6270	1152
Element size	dia 12 μm	Sq 100 μm	dia 74-90 μm	dia 25 μm	dia 60 μm	dia 32 μm	dia 100 μm	dia 160 μm	dia 80 μm
Pitch	36 μm	150 μm	–	–	75 μm	75 μm	–	214 μm	270 μm

* Only active material of membrane w/o additional layers

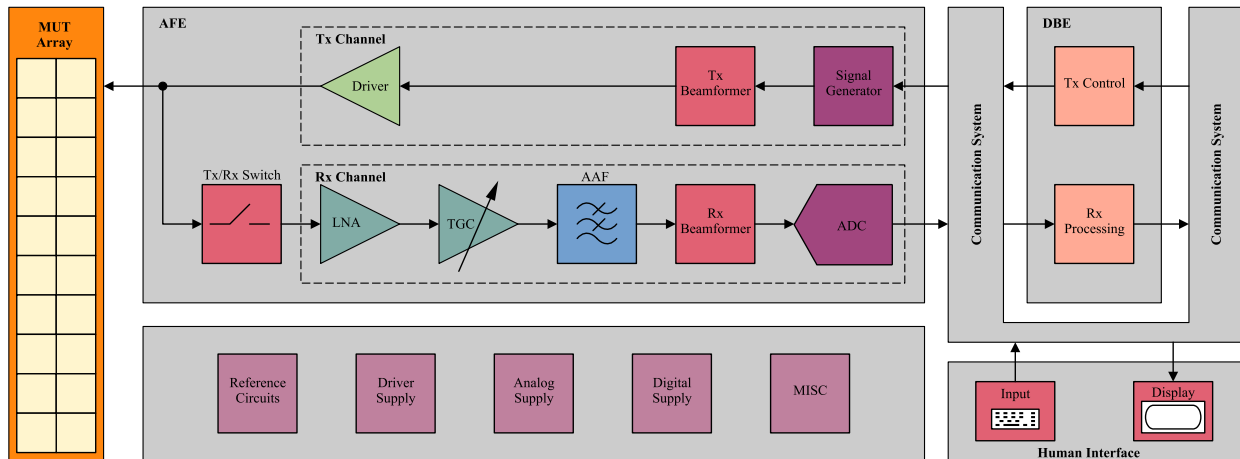


Fig. 2 Generalized ultrasound imaging system architecture

The number of signal paths in Tx/Rx channel can be larger than one and depends on the processing algorithm and number of array elements. AFE can be implemented as ASIC or set-up on PCB basis, while digital sub-system is usually either FPGA [34] or PC based [82] due to complicated algorithms. Examples of communication systems between the AFE and the DBE can include SPI, JESD (as a serial interface between data converters and FPGAs/ASICs), or LVDS [83]. Description of other most significant parts of the system is presented in the following sub-sections.

B. Excitation signal in Tx mode

In echo-based systems everything starts from the radiation of excitation wave, thus, the desirable high-efficient transfer of electrical power from the supply source to the ultrasonic transducer must occur. Such an excitation can be either achieved by tonal or square-wave electrical signals, depending on the application requirements, type and bandwidth of the transducer. For these purposes, driver circuit is used, which can be implemented as A- or AB-class power stages (pre-driven by a linear amplifiers) for tonal excitation [81], while level-shifter [84] circuits, also known as pulsers, implement square-wave excitation. Moreover, multi-level square-wave excitation can be used to improve power dissipation [85], [86], (so-called stepwise charging [87]), which is crucial for portable medical devices. Although pulsers are usually high-voltage (HV) circuits with high-side and low-side DMOS transistors controlled by gate drivers [88], the concept of using stacked low-voltage transistors was also presented [89], which helps to fabricate ASICs in standard CMOS technologies. From the wideband operation perspective, the bandwidths of transducer and driver have to be matched for obtaining optimal broadband transmitting and receiving characteristics, and also the pulser circuit should have low harmonic distortion, i.e., asymmetric square wave must be avoided. Therefore, the compensation of second-order harmonic (HD2) such as pulse inversion-cancellation method [90] should be used.

C. High-voltage isolation switch

The next crucial HV part of the system is a Tx/Rx switch, which enables isolation of sensitive and low-voltage receiving channel from high-voltage excitation signal coming out from the pulser. It must have low on-resistance (to maximize the input-output transfer ratio and to have better noise performance), low input parasitic capacitance (to reduce signal attenuation), and the ability to maintain bi-polar (positive and negative) isolation by using back-to-back connection. Hence, a variety of schematic implementations were developed, either simply utilizing of high-voltage MOSFETs [91] with impedance matching network, or using stacked low-voltage transistors [89], or bootstrapped [92] and gate floating [93] switches.

D. Signal preconditioning in Rx mode

After the acoustical power was transmitted into the body tissue, reflection occurs, and weak signals returned to the transducer array have to be amplified. However, since the amplitude of received signal depends on the distance traveled by the acoustic beam from the antenna to the reflecting surface and back (i.e. doubled distance), two requirements must be fulfilled: a) pre-amplification must be low-noisy and b) a compensation mechanism of differences in the near field (low-amplitude) and far field (high-amplitude) signals amplitude must be implemented (technically for different penetration depths), also known as the time-gain compensation/control (TGC) technique. The first requirement is satisfied in order to discriminate weak signals from the noisy background (i.e. the amplifier must have a satisfactory SNR), while the second condition is satisfied to adjust the signal in the input range of subsequent signal processing stage, typically ADC buffer — in other words, to protect ADC from overloading. So that, the former is done via low-noise amplifiers (LNA), while the latter is implemented via high dynamic range type of attenuation circuits like variable gain amplifiers (VGAs) or programmable gain amplifiers (PGAs) [94]. The difference

between these two architectures is that the gain changes either continuously (VGA) or in a discrete number of steps (PGA), and the choice between them is dictated by application requirements for a particular system, so different trade-offs have to be considered. Also, should be noted that LNA and VGA can be combined in order to realize a coarse/fine gain tuning [95], [96].

LNA are typically implemented as a transimpedance amplifier (TIA) [89], which serves as a first stage of current-to-voltage conversion. TIA needs to be impedance matched to the unit transducer with high output impedance [68], meaning that LNA requires to have low input impedance [97], and also needs to exhibit an excellent noise [98] and linearity performance [52]. One of the possible implementations of TIA was reported in [97] and consists of a single-ended common-source amplifier (further improved by cascode transistor in [98]) with a feedback resistor followed by a source follower, while TIA in [92] is using differential operational transconductance amplifier (OTA). TIA can be further followed by a second gain stage [68] or buffering circuits [52], [92], depending on the application needs.

Considering that the attenuation of ultrasound waves has an exponential dependence, the transfer function of the attenuation circuit (VGA or PGA) should be linear in the decibel scale. One example of this is reported in [95], where Padé approximation was used to obtain switched-capacitor VGA with signal continuity during gain transitions. Other implementations represent single-to-differential PGA with process-insensitive TGC gain, achieved by setting this gain by the load-to-differential pair transconductance ratio [98], or popular architecture of PGA with the feedback capacitors and OTA [92] or flipped voltage follower based push-pull amplifier [94]. Furthermore, the TGC algorithm requires an additional controlling circuit, which generates discrete or continuous control signal, and wide bandwidth of gain control loop is required to settle the attenuation path quickly, as well as high-impedance input and low noise requirements for such circuits should be satisfied [TGC]. Despite an algorithm of automatic adjustment of the TGC (ATGC) was proposed [99], in practice TGC control is usually done manually by operator, who chooses an appropriate TGC curve via sliders at interface board [100], since ATGC does not allow the full control over image quality due to differences of acoustic attenuation of different tissues and structures [101].

E. Analog-to-Digital Conversion

Robust digital processing is available only after the A/D conversion, therefore, ADC sub-module, with comes after the anti-aliasing filter (AAF) in the signal path (see Fig. 2), becomes crucial part of the data acquisition system. Among the main characteristics of ADCs, such as resolution (typically ~ 10 – 12 bit), conversion rate (typically ~ 20 MSps), signal-to-noise-and-distortion ratio (typically 50–70 dB) and sampling frequency (typically

~ 20 MHz), in the context of ultrasonic applications, another extremely important characteristic is the ability to process a huge number of channels, i.e. to allow multiplexing of a single ADC input between these channels, which helps to save the chip area. One example of such converter is a multichannel pipeline ADC with two parallel time-interleaved pipeline paths multiplexed into a single pipeline in order to decrease implementation efforts [102]. On the other hand, excellent accuracy can be achieved by using delta-sigma ADCs, but at the expense of area and increasing complexity of the system, for example, consisting from 128 processing channels [34] or implement digital integrator feedback (DIF) to reduce feedback DAC jitter impact [35]. These kinds of ADCs utilize complex topologies of high-order continuous-time Δ - Σ modulators, followed by the Cascaded Integrated Comb (CIC) and Finite Impulse Response (FIR) filters. A successive approximation register (SAR) ADCs [103] is another good choice for ultrasound integrated system because of their moderate area consumption and possibility of implementation in standard HV technology [92]. Alternative approach of A/D conversion, reported in [96], is to combine two types of ADCs — already mentioned SAR ADC as a first stage, followed by single-slope (SS) ADC as a second stage.

F. Beamforming algorithms and circuitry

As already was briefly mentioned, the arrays, called acoustic antennas, consist of transducers, which in turn create the resulting acoustic field based on the interference interaction between each of the transducers. For this, it is necessary to excite (in Tx mode) each transducer with an electrical signal with a certain amplitude and phase relative to other transducers in the array; in contrast, in the Rx mode it is necessary to process the received signals by varying their phases and amplitudes. Therefore, different types of beamforming techniques were developed [104], such as multi-line acquisition (MLA), multi-line transmission (MLT), plane and diverging wave imaging, and synthetic aperture, as well as the approaches called null subtraction imaging (NSI) and coherence beamforming. Almost all of these techniques are based on the delay-and-sum beamforming method, which needs to have a delay cell in each path from the transducer (or a subarray, i.e. a group of transducers), and the electrical adder for RX channel, while the summation in Tx mode is taking place in the media itself. Also, different amplitude distributions over the array, obtained by introduction of weighting coefficients in each Rx/Tx path, helps to suppress “sidelobes” on either side of the main beam [105], which referred as apodization technique. In addition, the deep neural networks-based algorithms adaptation into ultrasound image processing was reported in [104], allowing the suppression of off-axis scattering.

To ensure the practical implementation of the above-mentioned delay-and-sum beamforming algorithms,



various circuits with electrical combination of signals, namely analog and digital beamformers (ABF and DBF), are developed [106], [107]. The main difference between these two approaches is where the introduction of delay/weighting occurs — before (analog beamformer) or after (digital beamformer) the ADC/DAC. The former gives the speed of computation, but requires precise matching between delay cells [108], while with the latter the high-accuracy computations can be achieved. ABF usually consists of the cascaded-delay-cell type or the analog-memory type delay cells and typically requires high-frequency clock signal to achieve appropriate time delay resolution [109]. As example, the analog delay line for ABF from [110] uses a bunch of unit delay cells, each consisting of two sampling capacitors, two source-follower buffers and programmable switches, followed by the load capacitor, thus implementing the pipelined sample-and-hold architecture. It also uses a current-splitting method (CSM) to reduce power consumption, which is crucial characteristic in all BFs, since the amount of data to be processed is huge. A proposed in [111] FPGA-based digital beamformer employs a synthetic aperture beamforming (SAB) technique, implementing sequential processing using a single channel, which helps to decrease the device size, power and cost. Another configurable DBF [112] intends to decrease power consumption by computing the delays on-chip to exclude the external memories for delay storage. As a further search for area improvements, a hybrid beamformer (HBF) was also developed [113], which helps to decrease area consumption by reducing the number of ADCs. It consists from the first ABF stage, with sample-and-hold-type analog memory array and a summing amplifier, followed by the second DBF stage with eight ADCs and a FIFO-based delay-and-sum block. Another interesting approach, intended to reduce the area, is an in-pixel delta-sigma modulation (DSM) beamforming, reported in [95].

G. Miscellaneous circuitry

Complete signal processing system is not imaginable without different miscellaneous circuitries, such as power supply regulators, which include high-voltage driver supply for CMUT pulsers, low-voltage supply regulators for AFE and DBE, reference temperature-

independent circuits for ADC or TGC, etc. In case of ASIC-based ultrasound systems, a protection against electrostatic discharges (ESD) must be achieved via special high-voltage on-chip structures, as well as design-for-testability (DFT) features is crucial for safe and high-quality product.

CONCLUSIONS

In this paper a summary of medical ultrasound systems was presented, paying attention to the bandwidth of the transducers and their miniaturization, also taking into account the features of signal processing and generation sub-systems. The application of such systems is extremely wide and covers almost all areas of medical treatment, and also allows the creation of small portable devices for everyday carry. They have evolved over the past eight decades, starting with the use of primitive electroacoustic transducers made from natural piezo materials, later expanding to the use of synthetic piezoceramic materials with improved performance, and finally using MEMS technology to create miniaturized transducers — micromachined ultrasound transducers. They include capacitive (CMUT) and piezoelectrical (PMUT) types of devices, the use of which in medical systems is dictated by trade-offs between bandwidth, the ability to provide HV electric biasing, and biocompatibility of the materials used for their production. The production of PMUT and CMUT is similar in many respects, the main and most difficult task of which is to create a membrane with specified characteristics and an underlying cavity on a very small scale. Broadband operation of the signal paths, which is crucial for obtaining high-quality ultrasound images, is achieved both by methods of improving the characteristics of an individual transducer and the use of arrays of transducers, as well as careful design for low harmonic distortion in driving and receiving electrical circuits, including both analog and digital types. The use of beamforming algorithms and sub-systems in ultrasound arrays allows to achieve scanning in several dimensions, including beam focusing. In general, miniaturized US systems are promising devices that require high-end technologies and help to obtain excellent results in improving of humans' life.

REFERENCES

- [1] C. F. Dietrich *et al.*, "History of Ultrasound in Medicine from its birth to date (2022), on occasion of the 50 Years Anniversary of EFSUMB. A publication of the European Federation of Societies for Ultrasound In Medicine and Biology (EFSUMB), designed to record the historical development of medical ultrasound," *Med Ultrason*, vol. 24, no. 4, p. 434, Dec. 2022, DOI: 10.11152/mu-3757.
- [2] R. Manske, K. Podoll, A. Markowski, M. Watkins, L. Hayward, and M. Maitland, "Physical Therapists Use of Diagnostic Ultrasound Imaging in Clinical Practice: A Review of Case Reports," *Int J Sports Phys Ther*, vol. 18, no. 1, Feb. 2023, DOI: 10.26603/001c.68137.
- [3] T. H. Williamson and A. Harris, "Color Doppler ultrasound imaging of the eye and orbit," *Surv Ophthalmol*, vol. 40, no. 4, pp. 255–267, Jan. 1996, DOI: 10.1016/S0039-6257(96)82001-7.
- [4] G. S. Mintz, "Intravascular Imaging of Coronary Calcification and Its Clinical Implications," *JACC Cardiovasc Imaging*, vol. 8, no. 4, pp. 461–471, Apr. 2015, DOI: 10.1016/j.jcmg.2015.02.003.
- [5] C.-K. Chen, Y.-L. Wan, L.-C. Hsieh, and P.-H. Tsui, "Transmastoid Ultrasound Detection of Middle Ear Effusion and Its Association with Clinical Audiometric Tests," *Life*, vol. 12, no. 4, p. 599, Apr. 2022, DOI: 10.3390/life12040599.
- [6] Z. Hou *et al.*, "Ultrasound Computed Tomography Reflection Imaging with Coherence-Factor Beamforming for Breast Tumor Early Detection," *Mathematics*, vol. 12, no. 7, p. 1106, Apr. 2024, DOI: 10.3390/math12071106.



- [7] F. Recker, U. Gembruch, and B. Strizek, "Clinical Ultrasound Applications in Obstetrics and Gynecology in the Year 2024," *J Clin Med*, vol. 13, no. 5, p. 1244, Feb. 2024, DOI: 10.3390/jcm13051244.
- [8] K. J. Rittenhouse *et al.*, "Accuracy of portable ultrasound machines for obstetric biometry," *Ultrasound in Obstetrics & Gynecology*, vol. 63, no. 6, pp. 772–780, Jun. 2024, DOI: 10.1002/uog.27541.
- [9] M. A. Mekky, "Endoscopic ultrasound in gastroenterology: From diagnosis to therapeutic implications," *World J Gastroenterol*, vol. 20, no. 24, p. 7801, 2014, DOI: 10.3748/wjg.v20.i24.7801.
- [10] A. S. Terkawi, D. Karakitsos, M. Elbarbary, M. Blaivas, and M. E. Durieux, "Ultrasound for the Anesthesiologists: Present and Future," *The Scientific World Journal*, vol. 2013, no. 1, Jan. 2013, DOI: 10.1155/2013/683685.
- [11] F. Recker, F. Kipfmüller, A. Wittek, B. Strizek, and L. Winter, "Applications of Point-of-Care-Ultrasound in Neonatology: A Systematic Review of the Literature," *Life*, vol. 14, no. 6, p. 658, May 2024, DOI: 10.3390/life14060658.
- [12] "History of Medical Ultrasound," *Donald School Journal of Ultrasound in Obstetrics and Gynecology*, vol. 11, no. 2, pp. 91–100, Jun. 2017, DOI: 10.5005/jp-journals-10009-1509.
- [13] A. Carovac, F. Smajlovic, and D. Junuzovic, "Application of Ultrasound in Medicine," *Acta Informatica Medica*, vol. 19, no. 3, p. 168, 2011, DOI: 10.5455/aim.2011.19.168-171.
- [14] A. F. Kukuk, F. Scheling, R. Panzer, S. Emmert, and B. Roth, "Combined ultrasound and photoacoustic C-mode imaging system for skin lesion assessment," *Sci Rep*, vol. 13, no. 1, p. 17947, Oct. 2023, DOI: 10.1038/s41598-023-44919-5.
- [15] T. Saul, S. D. Siadecki, R. Berkowitz, G. Rose, D. Matilsky, and A. Sauler, "M-Mode Ultrasound Applications for the Emergency Medicine Physician," *J Emerg Med*, vol. 49, no. 5, pp. 686–692, Nov. 2015, DOI: 10.1016/j.jemermed.2015.06.059.
- [16] G. M. Lanza, "Ultrasound Imaging," *Invest Radiol*, vol. 55, no. 9, pp. 573–577, Sep. 2020, DOI: 10.1097/RLI.0000000000000679.
- [17] M. Eagle, "Doppler ultrasound - basics revisited," *British Journal of Nursing*, vol. 15, no. Sup2, pp. S24–S30, Jun. 2006, DOI: 10.12968/bjon.2006.15.Sup2.21238.
- [18] J. M. Bustillo, R. T. Howe, and R. S. Muller, "Surface micromachining for microelectromechanical systems," *Proceedings of the IEEE*, vol. 86, no. 8, pp. 1552–1574, 1998, DOI: 10.1109/5.704260.
- [19] Q. Zhu *et al.*, "A Piezoelectric Micro-Machined Ultrasonic Transducer Array Based on Flexible Substrate," in *2018 IEEE 13th Annual International Conference on Nano/Micro Engineered and Molecular Systems (NEMS)*, 2018, pp. 345–348, DOI: 10.1109/NEMS.2018.8556929.
- [20] J. F. Hou *et al.*, "An implantable piezoelectric ultrasound stimulator (ImPULS) for deep brain activation," *Nat Commun*, vol. 15, no. 1, p. 4601, Jun. 2024, DOI: 10.1038/s41467-024-48748-6.
- [21] K. A. Snook *et al.*, "Design, fabrication, and evaluation of high frequency, single-element transducers incorporating different materials," *IEEE Trans Ultrason Ferroelectr Freq Control*, vol. 49, no. 2, pp. 169–176, Feb. 2002, DOI: 10.1109/58.985701.
- [22] K. T. Dussik, "Über die Möglichkeit, hochfrequente mechanische Schwingungen als diagnostisches Hilfsmittel zu verwenden," *Gesellschaft für Neurol. und Psychiatr*, vol. 1, no. 1, pp. 153–168, Dec. 1942.
- [23] Q. Zhou, K. H. Lam, H. Zheng, W. Qiu, and K. K. Shung, "Piezoelectric single crystal ultrasonic transducers for biomedical applications," *Prog Mater Sci*, vol. 66, pp. 87–111, Oct. 2014, DOI: 10.1016/j.pmatsci.2014.06.001.
- [24] S. A. Naida, T. M. Zheliaskova, A. S. Naida, H. A. Kliushnichenko, and A. V. Damarad, "Methods for Calculating the Transfer Functions of Broadband Plate Piezoelectric Transducers with Transition Layers," *Journal of Nano- and Electronic Physics*, vol. 13, no. 6, pp. 06029-1-06029-6, 2021, DOI: 10.21272/jnep.13(6).06029.
- [25] Z. Zhang, L. Yang, X. Wang, H. Luo, and Y. Wang, "Synergistic Enhancement of Bandwidth and Sensitivity of Phased Array Ultrasonic Transducer With Novel Acoustic Mismatch Structure," *IEEE Trans Instrum Meas*, vol. 73, pp. 1–7, 2024, DOI: 10.1109/TIM.2024.3375407.
- [26] T. A. Whittingham, "Broadband transducers," *Eur Radiol*, vol. 9, no. S3, pp. S298–S303, Nov. 1999, DOI: 10.1007/PL00014060.
- [27] M. Chen-Glasser, P. Li, J. Ryu, and S. Hong, "Piezoelectric Materials for Medical Applications," in *Piezoelectricity - Organic and Inorganic Materials and Applications*, InTech, 2018.
- [28] J. Peng, Z. Hu, H. Tang, X. Chen, T. Wang, and S. Chen, "Fabrication and performance of a 10 MHz annular array based on PMN-PT single crystal for medical imaging," in *2013 IEEE International Ultrasonics Symposium (IUS)*, 2013, pp. 516–518, DOI: 10.1109/ULTSYM.2013.0134.
- [29] J. Schulze-Clewing, M. J. Eberle, and D. N. Stephens, "Miniaturized circular array [for intravascular ultrasound]," in *2000 IEEE Ultrasonics Symposium. Proceedings. An International Symposium (Cat. No.00CH37121)*, pp. 1253–1254, DOI: 10.1109/ULTSYM.2000.921550.
- [30] C. Chircov and A. M. Grumezescu, "Microelectromechanical Systems (MEMS) for Biomedical Applications," *Micromachines (Basel)*, vol. 13, no. 2, p. 164, Jan. 2022, DOI: 10.3390/mi13020164.
- [31] J. Lee *et al.*, "A 36-Channel Auto-Calibrated Front-End ASIC for a pMUT-Based Miniaturized 3-D Ultrasound System," *IEEE J Solid-State Circuits*, vol. 56, no. 6, pp. 1910–1923, Jun. 2021, DOI: 10.1109/JSSC.2021.3049560.
- [32] A. Bhuyan *et al.*, "A 32x32 integrated CMUT array for volumetric ultrasound imaging," in *2013 IEEE International Ultrasonics Symposium (IUS)*, 2013, pp. 545–548, DOI: 10.1109/ULTSYM.2013.0141.
- [33] X. Zhu, K. Vasanth, X. Xu, C. Smyth, and B. Rhoton, "Application based reliability assessment and qualification methodology for medical ICs," in *2011 International Reliability Physics Symposium*, 2011, pp. 3B.4.1-3B.4.8, DOI: 10.1109/IRPS.2011.5784482.
- [34] M. K. Chirala, P. Huynh, J. Ryu, and Y.-H. Kim, "A 128-ch $\Delta\Sigma$ ADC based mixed signal IC for full digital beamforming Wireless handheld Ultrasound imaging system," in *2015 37th Annual International Conference of the IEEE Engineering in Medicine and Biology Society (EMBC)*, 2015, pp. 1339–1342, DOI: 10.1109/EMBC.2015.7318616.
- [35] T.-C. Cheng and T.-H. Tsai, "CMOS Ultrasonic Receiver With On-Chip Analog-to-Digital Front End for High-Resolution Ultrasound Imaging Systems," *IEEE Sens J*, vol. 16, no. 20, pp. 7454–7463, Oct. 2016, DOI: 10.1109/JSEN.2016.2599580.
- [36] J. Kang *et al.*, "A System-on-Chip Solution for Point-of-Care Ultrasound Imaging Systems: Architecture and ASIC Implementation," *IEEE Trans Biomed Circuits Syst*, vol. 10, no. 2, pp. 412–423, Apr. 2016, DOI: 10.1109/TBCAS.2015.2431272.
- [37] D. Brennan and P. Galvin, "Evaluation of a Machine Learning Algorithm to Classify Ultrasonic Transducer Misalignment and Deployment Using TinyML," *Sensors*, vol. 24, no. 2, p. 560, Jan. 2024, DOI: 10.3390/s24020560.
- [38] U. Denmirici, O. Oralkan, J. A. Johnson, A. S. Ergun, M. Karaman, and B. T. Khuri-Yakub, "Capacitive micromachined ultrasonic transducer arrays for medical imaging: experimental results," in *2001 IEEE Ultrasonics Symposium. Proceedings. An International Symposium (Cat. No.01CH37263)*, pp. 957–960, DOI: 10.1109/ULTSYM.2001.991878.
- [39] A. Dauba *et al.*, "Evaluation of capacitive micromachined ultrasonic transducers for passive monitoring of microbubble-assisted ultrasound therapies," *J Acoust Soc Am*, vol. 148, no. 4, pp. 2248–2255, Oct. 2020, DOI: 10.1121/10.0002096.



- [40] H. Wang, Y. Ma, H. Yang, H. Jiang, Y. Ding, and H. Xie, "MEMS Ultrasound Transducers for Endoscopic Photoacoustic Imaging Applications," *Micromachines (Basel)*, vol. 11, no. 10, p. 928, Oct. 2020, DOI: 10.3390/mi11100928.
- [41] Y. Lu *et al.*, "Broadband piezoelectric micromachined ultrasonic transducers based on dual resonance modes," in *2015 28th IEEE International Conference on Micro Electro Mechanical Systems (MEMS)*, 2015, pp. 146–149, DOI: 10.1109/MEMSYS.2015.7050907.
- [42] S. H. Øygaard *et al.*, "Contrast-enhanced ultrasound imaging using capacitive micromachined ultrasonic transducers," *J Acoust Soc Am*, vol. 153, no. 3, pp. 1887–1897, Mar. 2023, DOI: 10.1121/10.0017533.
- [43] L. Wang, W. Zhu, Z. Wu, W. Liu, and C. Sun, "A Novel Broadband Piezoelectric Micromachined Ultrasonic Transducer with Resonant Cavity," in *2021 IEEE International Ultrasonics Symposium (IUS)*, 2021, pp. 1–4, DOI: 10.1109/IUS52206.2021.9593779.
- [44] G. G. Yaralioglu, A. S. Ergun, and A. Bozkurt, "Vertical cavity capacitive transducer," *J Acoust Soc Am*, vol. 149, no. 4, pp. 2137–2144, Apr. 2021, DOI: 10.1121/10.0003931.
- [45] B. Shieh, K. G. Sabra, and F. L. Degertekin, "Efficient Broadband Simulation of Fluid-Structure Coupling for Membrane-Type Acoustic Transducer Arrays Using the Multilevel Fast Multipole Algorithm," *IEEE Trans Ultrason Ferroelectr Freq Control*, vol. 63, no. 11, pp. 1967–1979, Nov. 2016, DOI: 10.1109/TUFFC.2016.2591920.
- [46] K. Smyth and S.-G. Kim, "Experiment and simulation validated analytical equivalent circuit model for piezoelectric micromachined ultrasonic transducers," *IEEE Trans Ultrason Ferroelectr Freq Control*, vol. 62, no. 4, pp. 744–765, Apr. 2015, DOI: 10.1109/TUFFC.2014.006725.
- [47] Y. Birjisi *et al.*, "Piezoelectric Micromachined Ultrasonic Transducers (PMUTs): Performance Metrics, Advancements, and Applications," *Sensors*, vol. 22, no. 23, p. 9151, Nov. 2022, DOI: 10.3390/s22239151.
- [48] T. Xu *et al.*, "Equivalent Circuit Models of Cell and Array for Resonant Cavity-Based Piezoelectric Micromachined Ultrasonic Transducer," *IEEE Trans Ultrason Ferroelectr Freq Control*, vol. 67, no. 10, pp. 2103–2118, Oct. 2020, DOI: 10.1109/TUFFC.2020.2993805.
- [49] E. Ledesma, A. Uranga, F. Torres, and N. Barniol, "Fully Integrated Pitch-Matched AlScN PMUT-on-CMOS Array for High-Resolution Ultrasound Images," *IEEE Sens J*, vol. 24, no. 10, pp. 15954–15966, May 2024, DOI: 10.1109/JSEN.2024.3385911.
- [50] T. Xu, D. Caponi, and Z. Da, "Enhancing Broadband Transmission Performance of Piezoelectric Micromachined Ultrasonic Transducers (PMUTs) via Electrical Matching Network," in *2023 IEEE International Ultrasonics Symposium (IUS)*, 2023, pp. 1–4, DOI: 10.1109/IUS51837.2023.10307481.
- [51] H. Wang, Y. Yu, Z. Chen, H. Yang, H. Jiang, and H. Xie, "Design and Fabrication of a Piezoelectric Micromachined Ultrasonic Transducer Array Based on Ceramic PZT," in *2018 IEEE SENSORS*, 2018, pp. 1–4, DOI: 10.1109/ICSENS.2018.8589693.
- [52] S. Sharma and T. Ytterdal, "Low noise front-end amplifier design for medical ultrasound imaging applications," in *2012 IEEE/IFIP 20th International Conference on VLSI and System-on-Chip (VLSI-SoC)*, 2012, pp. 12–17, DOI: 10.1109/VLSI-SoC.2012.7332069.
- [53] Di Fu *et al.*, "A novel method for fabricating 2-D array piezoelectric micromachined ultrasonic transducers for medical imaging," in *2009 18th IEEE International Symposium on the Applications of Ferroelectrics*, 2009, pp. 1–4, DOI: 10.1109/ISAF.2009.5307546.
- [54] O. Oralkan, S. T. Hansen, B. Bayram, G. G. Yaralioglu, A. S. Ergun, and B. T. Khuri-Yakub, "High-frequency CMUT arrays for high-resolution medical imaging," in *IEEE Ultrasonics Symposium*, 2004, pp. 399–402, DOI: 10.1109/ULTSYM.2004.1417747.
- [55] Y. Lu, A. Heidari, and D. A. Horsley, "A High Fill-Factor Annular Array of High Frequency Piezoelectric Micromachined Ultrasonic Transducers," *Journal of Microelectromechanical Systems*, vol. 24, no. 4, pp. 904–913, Aug. 2015, DOI: 10.1109/JMEMS.2014.2358991.
- [56] F. Pop *et al.*, "Zero-Power Acoustic Wake-Up Receiver Based on DMUT Transmitter, PMUTs Arrays Receivers and MEMS Switches for Intrabody Links," in *2019 20th International Conference on Solid-State Sensors, Actuators and Microsystems & Eurosensors XXXIII (TRANSDUCERS & EUROSENSORS XXXIII)*, 2019, pp. 150–153, DOI: 10.1109/TRANSDUCERS.2019.8808176.
- [57] H.-Y. Chen, Y.-S. Chan, T.-H. Hsu, M.-H. Li, and S.-S. Li, "A Single-Chip CMOS-MEMS CMUT Array Transceiver With Low Bias," in *2023 22nd International Conference on Solid-State Sensors, Actuators and Microsystems (Transducers)*, 2023, pp. 136–139, URL: <https://ieeexplore.ieee.org/document/10516927>.
- [58] S. Sadeghpour, M. Ingram, C. Wang, J. D'Hooge, and M. Kraft, "A \$128 \times 1\$ Phased Array Piezoelectric Micromachined Ultrasound Transducer (pMUT) for Medical Imaging," in *2021 21st International Conference on Solid-State Sensors, Actuators and Microsystems (Transducers)*, 2021, pp. 34–37, DOI: 10.1109/Transducers50396.2021.9495521.
- [59] Y. He, H. Wan, X. Jiang, and C. Peng, "Piezoelectric Micromachined Ultrasound Transducer Technology: Recent Advances and Applications," *Biosensors (Basel)*, vol. 13, no. 1, p. 55, Dec. 2022, DOI: 10.3390/bios13010055.
- [60] K. K. Park, O. Oralkan, and B. T. Khuri-Yakub, "A comparison between conventional and collapse-mode capacitive micromachined ultrasonic transducers in 10-MHz 1-D arrays," *IEEE Trans Ultrason Ferroelectr Freq Control*, vol. 60, no. 6, pp. 1245–1255, Jun. 2013, DOI: 10.1109/TUFFC.2013.2688.
- [61] B. Zhu, B. P. Tiller, A. J. Walker, A. J. Mulholland, and J. F. C. Windmill, "'Pipe Organ' Inspired Air-Coupled Ultrasonic Transducers With Broader Bandwidth," *IEEE Trans Ultrason Ferroelectr Freq Control*, vol. 65, no. 10, pp. 1873–1881, Oct. 2018, DOI: 10.1109/TUFFC.2018.2861575.
- [62] M. Pekař, W. U. Dittmer, N. Mihajlović, G. van Soest, and N. de Jong, "Frequency Tuning of Collapse-Mode Capacitive Micromachined Ultrasonic Transducer," *Ultrasonics*, vol. 74, pp. 144–152, Feb. 2017, DOI: 10.1016/j.ultras.2016.10.002.
- [63] T. Wang and C. Lee, "Electrically switchable multi-frequency piezoelectric micromachined ultrasonic transducer (pMUT)," in *2016 IEEE 29th International Conference on Micro Electro Mechanical Systems (MEMS)*, 2016, pp. 1106–1109, DOI: 10.1109/MEMSYS.2016.7421828.
- [64] T. M. Adams and R. A. Layton, *Introductory MEMS*. Boston, MA: Springer US, 2010, ISBN: 978-0-387-09510-3.
- [65] A. Dangi *et al.*, "A Photoacoustic Imaging Device Using Piezoelectric Micromachined Ultrasound Transducers (PMUTs)," *IEEE Trans Ultrason Ferroelectr Freq Control*, vol. 67, no. 4, pp. 801–809, Apr. 2020, DOI: 10.1109/TUFFC.2019.2956463.
- [66] X.-B. Wang *et al.*, "Development of Broadband High-Frequency Piezoelectric Micromachined Ultrasonic Transducer Array," *Sensors*, vol. 21, no. 5, p. 1823, Mar. 2021, DOI: 10.3390/s21051823.
- [67] S. Sadeghpour, S. V. Joshi, C. Wang, and M. Kraft, "Novel Phased Array Piezoelectric Micromachined Ultrasound Transducers (pMUTs) for Medical Imaging," *IEEE Open Journal of Ultrasonics, Ferroelectrics, and Frequency Control*, vol. 2, pp. 194–202, 2022, DOI: 10.1109/OJUFFC.2022.3207128.
- [68] W. Ji *et al.*, "Total-Focus Ultrasonic Imaging of Defects in Solids Using a PZT Piezoelectric Micromachined Ultrasonic Transducer Array," *IEEE Trans Ultrason Ferroelectr Freq Control*, vol. 68, no. 4, pp. 1380–1386, Apr. 2021, DOI: 10.1109/TUFFC.2020.3032988.
- [69] Q. Zhou, S. Lau, D. Wu, and K. Kirk Shung, "Piezoelectric films for high frequency ultrasonic transducers in biomedical applications," *Prog Mater Sci*, vol. 56, no. 2, pp. 139–174, Feb. 2011, DOI: 10.1016/j.pmatsci.2010.09.001.

- [70] L. Zhao, C. Yang, X. Zhang, Z. You, and Y. Lu, "Broadband and High-Pressure Output PMUT Array Based on Lead-Free KNN Thin Film," in *2024 IEEE 37th International Conference on Micro Electro Mechanical Systems (MEMS)*, 2024, pp. 979–982, DOI: 10.1109/MEMS58180.2024.10439309.
- [71] W. Liu, C. Zhu, and D. Wu, "Flexible piezoelectric micro ultrasonic transducer array integrated on various flexible substrates," *Sens Actuators A Phys*, vol. 317, p. 112476, Jan. 2021, DOI: 10.1016/j.sna.2020.112476.
- [72] Z. Wang *et al.*, "Fabrication of 2-D Capacitive Micromachined Ultrasonic Transducer (CMUT) Array through Silicon Wafer Bonding," *Micromachines (Basel)*, vol. 13, no. 1, p. 99, Jan. 2022, DOI: 10.3390/mi13010099.
- [73] D. H. Le, T. Manh, and L. Hoff, "Lamination of Capacitive Micromachined Ultrasonic Transducer on a Piezoelectric Array: Process and Evaluation," in *2023 24th European Microelectronics and Packaging Conference & Exhibition (EMPC)*, 2023, pp. 1–4, DOI: 10.23919/EMPC55870.2023.10418279.
- [74] A. Caronti *et al.*, "Capacitive micromachined ultrasonic transducer (CMUT) arrays for medical imaging," *Microelectronics J*, vol. 37, no. 8, pp. 770–777, Aug. 2006, DOI: 10.1016/j.mejo.2005.10.012.
- [75] K. Brenner, A. Ergun, K. Firouzi, M. Rasmussen, Q. Stedman, and B. Khuri-Yakub, "Advances in Capacitive Micromachined Ultrasonic Transducers," *Micromachines (Basel)*, vol. 10, no. 2, p. 152, Feb. 2019, DOI: 10.3390/mi10020152.
- [76] Y. Qiu *et al.*, "Piezoelectric Micromachined Ultrasound Transducer (PMUT) Arrays for Integrated Sensing, Actuation and Imaging," *Sensors*, vol. 15, no. 4, pp. 8020–8041, Apr. 2015, DOI: 10.3390/s150408020.
- [77] A. Ivanov and U. Mescheder, "Surface Micromachining (Sacrificial Layer) and Its Applications in Electronic Devices," in *Porous Silicon: From Formation to Applications: Optoelectronics, Microelectronics, and Energy Technology Applications*, 1st ed., vol. 3, CRC Press, Taylor & Francis Group, LLC, 2016, pp. 129–141.
- [78] O. V. Korzyk, V. S. Didkovskiy, O. H. Leiko, O. M. Petryshchev, S. A. Naida, and S. M. Poroshyn, *Akustychni anteny. Navchal'nyy posibnyk [Acoustic antennas. Study guide]*. Kyiv, Ukraine: NTUU "KPI," 2013.
- [79] A. Hajati *et al.*, "Three-dimensional micro electromechanical system piezoelectric ultrasonic transducer," *Appl Phys Lett*, vol. 101, no. 25, Dec. 2012, DOI: 10.1063/1.4772469.
- [80] K. Suzuki, Y. Nakayama, N. Shimizu, and T. Mizuno, "Study on Wide-Band Piezoelectric Micro-Machined Ultrasound Transducers (pMUT) by Combined Resonance Frequencies and Controlling Poling Directions," in *2018 IEEE International Ultrasonics Symposium (IUS)*, 2018, pp. 1–3, DOI: 10.1109/ULTSYM.2018.8579949.
- [81] K. Sun *et al.*, "A 180-V_{pp} Integrated Linear Amplifier for Ultrasonic Imaging Applications in a High-Voltage CMOS SOI Technology," *IEEE Transactions on Circuits and Systems II: Express Briefs*, vol. 62, no. 2, pp. 149–153, Feb. 2015, DOI: 10.1109/TCSII.2014.2387687.
- [82] T. Kim *et al.*, "Design of an Ultrasound Transceiver ASIC with a Switching-Artifact Reduction Technique for 3D Carotid Artery Imaging," *Sensors*, vol. 21, no. 1, p. 150, Dec. 2020, DOI: 10.3390/s21010150.
- [83] "AFE58JD18 16-Channel, Ultrasound AFE with 14-Bit, 65-MSPS or 12-Bit, 80-MSPS ADC, Passive CW Mixer, I/Q Demodulator, and LVDS, JESD204B Outputs." Texas Instruments, May-2016, URL: <https://www.ti.com/lit/gpn/AFE58JD18>.
- [84] M. J. Declercq, M. Schubert, and F. Clement, "5 V-to-75 V CMOS output interface circuits," in *1993 IEEE International Solid-State Circuits Conference Digest of Technical Papers*, 1993, pp. 162–163, DOI: 10.1109/ISSCC.1993.280014.
- [85] G. Jung, C. Tekes, A. Pirouz, F. L. Degertekin, and M. Ghovanloo, "Supply-Doubled Pulse-Shaping High Voltage Pulser for CMUT Arrays," *IEEE Transactions on Circuits and Systems II: Express Briefs*, vol. 65, no. 3, pp. 306–310, Mar. 2018, DOI: 10.1109/TCSII.2017.2691676.
- [86] K. Chen, H.-S. Lee, A. P. Chandrakasan, and C. G. Sodini, "Ultrasonic Imaging Transceiver Design for CMUT: A Three-Level 30-V_{pp} Pulse-Shaping Pulser With Improved Efficiency and a Noise-Optimized Receiver," *IEEE J Solid-State Circuits*, vol. 48, no. 11, pp. 2734–2745, Nov. 2013, DOI: 10.1109/JSSC.2013.2274895.
- [87] L. J. Svensson and J. G. Koller, "Driving a capacitive load without dissipating fCV/sup 2/," in *Proceedings of 1994 IEEE Symposium on Low Power Electronics*, 1994, pp. 100–101, DOI: 10.1109/LPE.1994.573220.
- [88] A. S. Savoia *et al.*, "An ultra-low-power fully integrated ultrasound imaging CMUT transceiver featuring a high-voltage unipolar pulser and a low-noise charge amplifier," in *2014 IEEE International Ultrasonics Symposium*, 2014, pp. 2568–2571, DOI: 10.1109/ULTSYM.2014.0641.
- [89] A. Banuaji and H.-K. Cha, "A 15-V Bidirectional Ultrasound Interface Analog Front-End IC for Medical Imaging Using Standard CMOS Technology," *IEEE Transactions on Circuits and Systems II: Express Briefs*, vol. 61, no. 8, pp. 604–608, Aug. 2014, DOI: 10.1109/TCSII.2014.2327455.
- [90] "4-Channel Integrated Ultrasound Pulser HV7321 Second Harmonic Distortion Measurement." Microchip Technology Inc., 2016, URL: <https://ww1.microchip.com/downloads/aemDocuments/documents/OTH/ApplicationNotes/ApplicationNotes/00002303A.pdf>.
- [91] W. T. Ang, C. Scurtescu, W. Hoy, T. El-Bialy, Y. Y. Tsui, and J. Chen, "Design and Implementation of Therapeutic Ultrasound Generating Circuit for Dental Tissue Formation and Tooth-Root Healing," *IEEE Trans Biomed Circuits Syst*, vol. 4, no. 1, pp. 49–61, Feb. 2010, DOI: 10.1109/TBCAS.2009.2034635.
- [92] M. Tan *et al.*, "A Front-End ASIC With High-Voltage Transmit Switching and Receive Digitization for 3-D Forward-Looking Intravascular Ultrasound Imaging," *IEEE J Solid-State Circuits*, vol. 53, no. 8, pp. 2284–2297, Aug. 2018, DOI: 10.1109/JSSC.2018.2828826.
- [93] J. S. Kenji Hara, "A New 80V 32x32ch Low Loss Multiplexer LSI for a 3D Ultrasound Imaging System," in *Proceedings. ISPSD '05. The 17th International Symposium on Power Semiconductor Devices and ICs, 2005.*, pp. 359–362, DOI: 10.1109/ISPSD.2005.1488025.
- [94] M.-H. Son, Y.-C. Lee, H.-M. Baek, H.-J. Choi, and J.-Y. Um, "A Programmable Gain Amplifier with Fast Transient Response for Medical Ultrasound System," in *2022 19th International SoC Design Conference (ISOCC)*, 2022, pp. 302–303, DOI: 10.1109/ISOCC56007.2022.10031342.
- [95] M.-C. Chen *et al.*, "A Pixel Pitch-Matched Ultrasound Receiver for 3-D Photoacoustic Imaging With Integrated Delta-Sigma Beamformer in 28-nm UTBB FD-SOI," *IEEE J Solid-State Circuits*, pp. 1–14, 2017, DOI: 10.1109/JSSC.2017.2749425.
- [96] Y. M. Hopf *et al.*, "A Pitch-Matched High-Frame-Rate Ultrasound Imaging ASIC for Catheter-Based 3-D Probes," *IEEE J Solid-State Circuits*, vol. 59, no. 2, pp. 476–491, Feb. 2024, DOI: 10.1109/JSSC.2023.3299749.
- [97] I. O. Wygant *et al.*, "Integration of 2D CMUT arrays with front-end electronics for volumetric ultrasound imaging," *IEEE Trans Ultrason Ferroelectr Freq Control*, vol. 55, no. 2, pp. 327–342, Feb. 2008, DOI: 10.1109/TUFFC.2008.652.
- [98] F. U. Putri and H.-K. Cha, "A low-power low-noise ultrasonic receiver front-end IC for medical imaging systems," in *2017 International SoC Design Conference (ISOCC)*, 2017, pp. 318–319, DOI: 10.1109/ISOCC.2017.8368916.
- [99] R. Moshavegh *et al.*, "Automated hierarchical time gain compensation for *in-vivo* ultrasound imaging," 2015, p. 941904, DOI: 10.1117/12.2081619.



- [100] K. Yoon, "Ultrasound diagnosis apparatus and time gain compensation (TGC) setting method performed by the ultrasound diagnosis apparatus," EP 2 865 338 A1, 29-Apr-2015.
- [101] G. Vara, A. Rustici, A. Sechi, C. Mosconi, V. Lucidi, and R. Golfieri, "Texture analysis on ultrasound: The effect of time gain compensation on histogram metrics and gray-level matrices," *J Med Phys*, vol. 45, no. 4, p. 249, 2020, DOI: 10.4103/jmp.JMP_82_20.
- [102] K. Kaviani, O. Oralkan, P. Khuri-Yakub, and B. A. Wooley, "A multichannel pipeline analog-to-digital converter for an integrated 3-D ultrasound imaging system," *IEEE J Solid-State Circuits*, vol. 38, no. 7, pp. 1266–1270, Jul. 2003, DOI: 10.1109/JSSC.2003.813294.
- [103] B. Malki, T. Yamamoto, B. Verbruggen, P. Wambacq, and J. Craninckx, "A 70 dB DR 10 b 0-to-80 MS/s Current-Integrating SAR ADC With Adaptive Dynamic Range," *IEEE J Solid-State Circuits*, vol. 49, no. 5, pp. 1173–1183, May 2014, DOI: 10.1109/JSSC.2014.2309086.
- [104] L. Demi, "Practical Guide to Ultrasound Beam Forming: Beam Pattern and Image Reconstruction Analysis," *Applied Sciences*, vol. 8, no. 9, p. 1544, Sep. 2018, DOI: 10.3390/app8091544.
- [105] T. L. Szabo, *Diagnostic Ultrasound Imaging: Inside Out*, 2nd ed. Elsevier, 2014, ISBN: 9780123964878.
- [106] T. Halvorsrod, W. Luzzi, and T. S. Lande, "A log-domain μ /beamformer for medical ultrasound imaging systems," *IEEE Transactions on Circuits and Systems I: Regular Papers*, vol. 52, no. 12, pp. 2563–2575, Dec. 2005, DOI: 10.1109/TCSI.2005.857544.
- [107] T. K. Song and J. F. Greenleaf, "Ultrasonic dynamic focusing using an analog FIFO and asynchronous sampling," *IEEE Trans Ultrason Ferroelectr Freq Control*, vol. 41, no. 3, pp. 326–332, May 1994, DOI: 10.1109/58.285466.
- [108] J. R. Talman, S. L. Garverick, and G. R. Lockwood, "Integrated circuit for high-frequency ultrasound annular array," in *Proceedings of the IEEE 2003 Custom Integrated Circuits Conference, 2003.*, pp. 477–480, DOI: 10.1109/CICC.2003.1249444.
- [109] J.-Y. Um *et al.*, "A Single-Chip 32-Channel Analog Beamformer With 4-ns Delay Resolution and 768-ns Maximum Delay Range for Ultrasound Medical Imaging With a Linear Array Transducer," *IEEE Trans Biomed Circuits Syst*, vol. 9, no. 1, pp. 138–151, Feb. 2015, DOI: 10.1109/TBCAS.2014.2325851.
- [110] J.-Y. Jeong, J.-S. An, S.-J. Jung, S.-K. Hong, and O.-K. Kwon, "A Low-Power Analog Delay Line Using a Current-Splitting Method for 3-D Ultrasound Imaging Systems," *IEEE Transactions on Circuits and Systems II: Express Briefs*, vol. 65, no. 7, pp. 829–833, Jul. 2018, DOI: 10.1109/TCSII.2017.2717042.
- [111] G. Peyton, B. Farzaneh, H. Soleimani, M. G. Boutelle, and E. M. Drakakis, "Quadrature Synthetic Aperture Beamforming Front-End for Miniaturized Ultrasound Imaging," *IEEE Trans Biomed Circuits Syst*, vol. 12, no. 4, pp. 871–883, Aug. 2018, DOI: 10.1109/TBCAS.2018.2836915.
- [112] P. A. Hager, A. Bartolini, and L. Benini, "Ekho: A 30.3W, 10k-Channel Fully Digital Integrated 3-D Beamformer for Medical Ultrasound Imaging Achieving 298M Focal Points per Second," *IEEE Trans Very Large Scale Integr VLSI Syst*, vol. 24, no. 5, pp. 1936–1949, May 2016, DOI: 10.1109/TVLSI.2015.2488020.
- [113] J.-Y. Um *et al.*, "An Analog-Digital Hybrid RX Beamformer Chip With Non-Uniform Sampling for Ultrasound Medical Imaging With 2D CMUT Array," *IEEE Trans Biomed Circuits Syst*, vol. 8, no. 6, pp. 799–809, Dec. 2014, DOI: 10.1109/TBCAS.2014.2375958.

Надійшла до редакції 08 червня 2024 року

Прийнята до друку 14 серпня 2024 року




Огляд мікрофабрикованих ультразвукових систем для біомедичних застосувань

Р. Ю. Костюк^f,  [0009-0006-9575-2599](https://orcid.org/0009-0006-9575-2599)

С. А. Найда^s, д-р техн. наук проф,  [0000-0002-5060-2929](https://orcid.org/0000-0002-5060-2929)

Національний технічний університет України

«Київський політехнічний інститут імені Ігоря Сікорського»  [00syn5v21](https://doi.org/10.20535/2523-4455.me.303514)

Київ, Україна

Анотація—Використання ультразвуку (УЗ) в медичній промисловості інтенсивно розвивалося протягом останніх восьми десятиліть, і наразі різноманітність медичних застосувань включає широкий спектр діагностичних можливостей, які задовольняють вимогам загальної фізичної діагностики, офтальмології, кардіології, отоларингології, онкології, акушерства та гінекології, гастроентерології, анестезіології тощо.

Технології, які використовуються в медичному ультразвуковому дослідженні, рухалися вперед від простих одновимірних сканерів до складних систем візуалізації, а також мініатюризованих носимих або імплантованих ультразвукових датчиків.

П'єзоелектричні матеріали стали стандартом у медичному ультразвуковому діагностуванні. Цій технології притаманний ряд особливостей, а саме необхідність узгодження імпедансів та вимоги до розширення робочого діапазону частот системи. Перше призводить до втрат потужності під час передачі акустичної енергії, тоді як друге має вирішальне значення для забезпечення якісної роздільної здатності і, як наслідок, впливає на деталізацію опису уражень або анатомічних особливостей органів людини. Іншим аспектом є сумісність з біологічними тканинами, що призвело до різноманітних синтезованих п'єзокерамічних матеріалів.

Одночасно із розвитком п'єзоелектричних матеріалів, відбулось розширення можливостей мікроелектронного виробництва, що спричинило прорив у розробці ультразвукових перетворювачів завдяки винаходу так званих мікрооброблених ультразвукових перетворювачів (МУП). Такі перетворювачі є багатообіцяючою технологією, яка може допомогти досягти ряду переваг порівняно зі звичайними п'єзокерамічними пристроями, таких як сумісність з платформами спеціалізованих інтегральних мікросхем, внаслідок чого підвищується загальна надійність електронної системи, а також мінімізація проблем, пов'язаних з безпекою пацієнтів. Вони також забезпечують можливість зменшити енергоспоживання системи за допомогою складної енергоефективної схеми обробки і покращити узгодження імпедансів. Ще одна перевага МУП полягає в тому, що вони мають кращу відповідність між елементами ультразвукового масиву саме завдяки повторюваності технологій виготовлення.

Ультразвукові системи візуалізації зазвичай включають не лише один перетворювач, а цілий їх масив, інтегрований в акустичну антену. У таких системах алгоритми формування УЗ променя виконуються шляхом введення затримок в тракти передачі або прийому електричних сигналів для кожного перетворювача (або їх групи) в масиві. Такі підходи можуть дати перевагу в отриманні ширшої смуги пропускання методами перекриття частотного спектру кількох перетворювачів з різними формами мембрани або формуванням одного каналу, який включає перетворювачі із суміжними резонансними частотами.

Електрична частина ультразвукової системи зазвичай складається трактів попередньої аналогової обробки і кінцевої цифрової обробки сигналів. Перший тракт слугує для накачування потужності в режимі випромінювання і попереднього підсилення відбитого сигналу в режимі прийому, тому включає в себе схеми драйверів, низькошумних підсилювачів, аналогових фільтрів та аналогово-цифрових перетворювачів (АЦП). Другий тракт використовується для керування режимами роботи АЦП і реалізує загальний алгоритм цифрової обробки сигналу. Засоби формування направленості у режимах прийому та випромінювання можуть бути реалізовані як цифровими, так і аналоговими методами.

Отже, у статті досліджено принципи розробки та виготовлення мікрооброблених ультразвукових перетворювачів, а також визначено основні принципи побудови аналогово-цифрових систем обробки сигналів, акцентуючи увагу на забезпеченні широкосмуговості пристроїв трактів прийому та передачі.

Ключові слова — біомедичне УЗД; широкосмугові перетворювачі; мікромашинні ультразвукові перетворювачі (MUTs); CMUT; PMUT; ASIC; CMOS.

